DOI: 10.1002/cmdc.200600246

Potent Inhibitors of the Human UDP-Glucuronosyltransferase 2B7 Derived from the Sesquiterpenoid Alcohol Longifolol

Ingo Bichlmaier,[a] Mika Kurkela,[b] Tanmaya Joshi,[c] Antti Siiskonen,[a] Tobias Rüffer,[d] Heinrich Lang,[d] Moshe Finel,[b] and Jari Yli-Kauhaluoma*[a]

The tricyclic sesquiterpenol (+)-longifolol served as a lead structure for the design of inhibitors of the human UDP-glucuronosyltransferase (UGT) 2B7. Twenty-four homochiral and epimeric longifolol derivatives were synthesized and screened for their ability to inhibit the enzyme. The absolute configuration at the stereogenic center C1′ was determined by X-ray crystallography and 2D NMR spectroscopy (gHSQC, gNOESY). The phenyl-substituted secondary alcohol ***16b*** *(β-phenyllongifolol) displayed the highest affinity toward UGT2B7, and its inhibitory dissociation constant was 0.91 nM. The mode of inhibition was rapidly reversible and competitive. The inhibitor was not glucuronidated by UGT2B7 or other hepatic UGTs, presumably as a result of the high steric demand exerted by the phenyl group. Inhibition assays employing 14 other UGT isoforms suggested that inhibitor* ***16b*** *was highly selective for UGT2B7.*

Introduction

The UDP-glucuronosyltransferases (UGTs, EC 2.4.1.17) belong to the phase II metabolic system of the human body and catalyze the transfer of glucuronic acid (GlcA) from UDP-α-D-glucuronic acid (UDPGlcA) to lipophilic endobiotics and xenobiotics. This conjugation reaction is a major detoxification pathway, and many drugs are metabolized by these enzymes.[1] Eighteen UGT isoforms belonging either to subfamily 1A or 2B have been described,[2] but merely seven UGT enzymes are assumed to be involved in the conjugation of drugs.[3] The single most important UGT enzyme responsible for drug glucuronidation is presumably UGT2B7, which catalyzes the glucuronidation of ~40% of drugs that are metabolized by UGT enzymes.[3]

Metabolic enzymes are commonly described to possess a high degree of flexibility, or promiscuity, to depict their complex and partly overlapping substrate selectivities.[4] These enzymes apparently evolved to possess broad substrate selectivities so that they can detoxify a wide range of structurally different compounds.[5] The detailed reaction mechanism of the enzymatic glucuronidation reaction has not been determined to date, and the X-ray crystal structure of any of the UGT isoforms is yet to be resolved. However, the UGT-catalyzed conjugation reaction proceeds with inversion of configuration at the anomeric carbon atom of GlcA to afford exclusively β-D-glucuronides, and it is therefore assumed that the reaction resembles the bimolecular nucleophilic substitution reaction (S_N2). Prominent enzymes that stabilize the gas-phase transition state of an S_N2 displacement reaction are, for example, haloalkane dehalogenase of *Xanthobacter autotrophicus* and *S*-adenosylmethionine synthetase.[6]

Isoform-selective and potent inhibitors of metabolic enzymes are important for pharmacokinetic studies in drug design and development.[7] Selective inhibitors can be used to identify the enzymes responsible for the transformation of drugs and can be applied to testing in human tissue. Furthermore, they can be used to elucidate drug–drug interactions and for the detection of enzyme polymorphism.[4] Some inhibitors of UGT enzymes have been described, but most of them lack desirable levels of isoform selectivity and potency.[8] Even transition state (TS) mimics for UGT enzymes have been proposed.[9] However, these inhibitors lack the expected high affinity and specificity levels that are commonly associated with TS analogues. This is probably due to the shortfall to elucidate TS-defining properties such as bond lengths, bond angles, and electrostatic potential surfaces.[10] Many attempts for the design of UGT inhibitors and TS analogues were based on the preparation of bisubstrate analogues by attaching a UDP-like moiety to a lipophilic aglycone-like entity.[11] These approaches

[a] *I. Bichlmaier, A. Siiskonen, Prof. J. Yli-Kauhaluoma*
Division of Pharmaceutical Chemistry, University of Helsinki
P.O. Box 56, 00014 Helsinki (Finland)
Fax: (+358) 9-19159556
E-mail: jari.yli-kauhaluoma@helsinki.fi

[b] *M. Kurkela, Dr. M. Finel*
Drug Discovery and Development Technology Center, University of Helsinki
P.O. Box 56, 00014 Helsinki (Finland)

[c] *T. Joshi*
Department of Chemistry, Indian Institute of Technology
Kanpur 208016 (India)

[d] *Dr. T. Rüffer, Prof. H. Lang*
Lehrstuhl für Anorganische Chemie, Technische Universität Chemnitz
Straße der Nationen 62, 09111 Chemnitz (Germany)

Supporting information for this article is available on the WWW under http://www.chemmedchem.org or from the author.

did not result in the development of either potent UGT inhibitors or the derivation of applicable structure–activity relationships that could be used for further inhibitor design.

However, a random-screening approach has recently shown that hecogenin is presumably an isoform-selective inhibitor for UGT1A4.[12] The design of UGT inhibitors based on rational principles such as detailed structure–activity relationships employing whole series of compounds has been rarely conducted.

The design of potent and isoform-selective inhibitors for UGT enzymes is challenging because no crystal structure of any of the UGT enzymes has been resolved, and hence, computational approaches to derive lead compounds cannot be applied. Furthermore, the development of selective inhibitors for UGT enzymes is difficult owing to their inherent overlapping substrate selectivities, and only some isoform-selective substrates for UGTs have been identified.[4] This lack of data prevents the derivation of pharmacophores to develop isoform-selective lead compounds. Yet another obstacle in the development of inhibitors is that common functional groups which promote water solubility, such as hydroxy, amino, thiol, and carboxy groups, serve as nucleophiles in the enzymatic glucuronidation reaction. Therefore, inhibitors that possess such chemical functionalities may turn out to be substrates. Moreover, UGTs in general exert low affinities toward their substrates, which renders it difficult to identify structural features that result in high potency.[3]

We have recently shown that the epimeric sesquiterpenols cedrol, epicedrol, longifolol (**1**), and isolongifolol displayed high affinities toward UGT2B7.[13] Furthermore, the rate of the enzymatic glucuronidation reaction was significantly controlled by steric and stereochemical features, whereas the affinities were not influenced by these properties.[14] These results might therefore provide a rational approach for the design of inhibitors by addressing steric and stereochemical features to turn high-affinity substrates into true inhibitors. The tricyclic sesquiterpenol longifolol displayed a low inhibitory dissociation constant of 23 nM, and it was therefore chosen as the lead compound for this study. Twenty-four derivatives of longifolol were synthesized and screened for their ability to inhibit the human UGT2B7 (Figure 1).

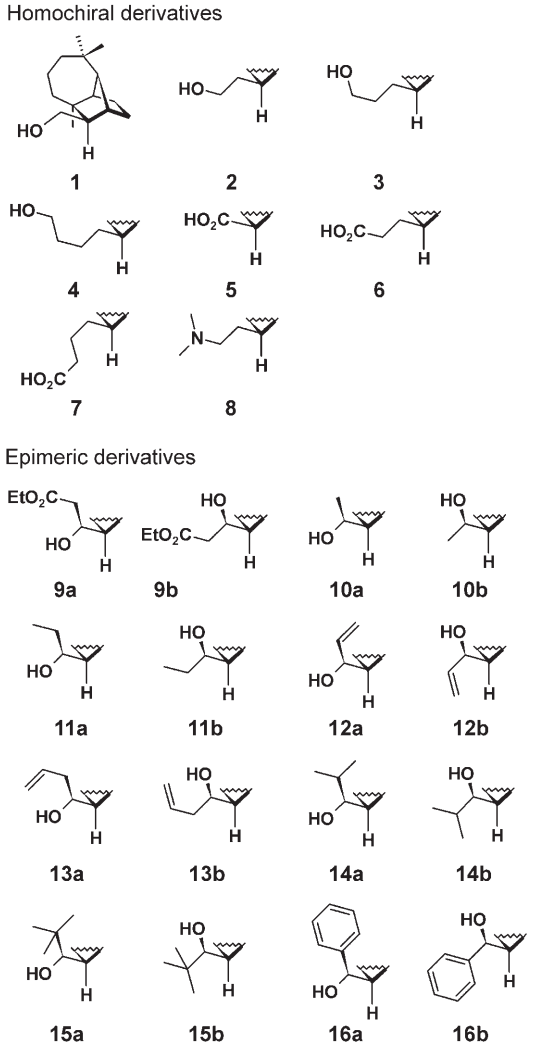

Figure 1. Homochiral and epimeric longifolol derivatives. The epimers that eluted faster from the chromatography column are denoted by **a**, the slower-eluting stereoisomers by **b**. All the faster-eluting compounds display the same relative configurations as do the slower-eluting compounds, with the exception of the *tert*-butyl derivatives **15a** and **15b**. For the latter, the relative configuration is inversed (see below).

Results and Discussion

Syntheses

Two sets of compounds were prepared from the common precursor (+)-longifolene,[15] and they possess the chiral tricyclo[5.4.0.0^{2,9}]undecane framework, which holds five asymmetric carbon atoms at the positions 1, 2, 7, 8, and 9 in the tricyclic scaffold (the numbering of the carbon atoms is displayed in the Supporting Information). The first series comprised homochiral homologous primary alcohols, carboxylic acids, and one tertiary amine (Figure 1, compounds **1**–**8**) to investigate the effect of these functional groups on the affinity toward UGT2B7 as a function of their distance from the hydrocarbon tricycle. The second set of epimeric secondary alcohols bearing various lipophilic substituents of varying size at the stereogenic center C1′ was prepared to analyze the influence of the spatial arrangement and the steric bulk of the substituents on the inhibition levels.

The aldehyde **17** was an important precursor for the preparation of the longifolol derivatives (Scheme 1) and was conveniently synthesized by the use of 2-iodoxybenzoic acid (IBX) as the oxidant,[16] which afforded the aldehyde in quantitative yield and high purity after aqueous workup. The diastereomeric β-hydroxy esters **9a** and **9b** were synthesized under mild conditions by titanocene-promoted Reformatsky reaction, employing ethyl bromoacetate and manganese, in excellent yields.[17] The use of zinc dust as a reducing agent caused byproduct formation, and the yields of the epimeric β-hydroxy esters were only moderate. The alkyl-substituted epimeric secondary alcohols **10a**–**16b** were prepared by Grignard reaction employing 5 equivalents of the corresponding Grignard re-

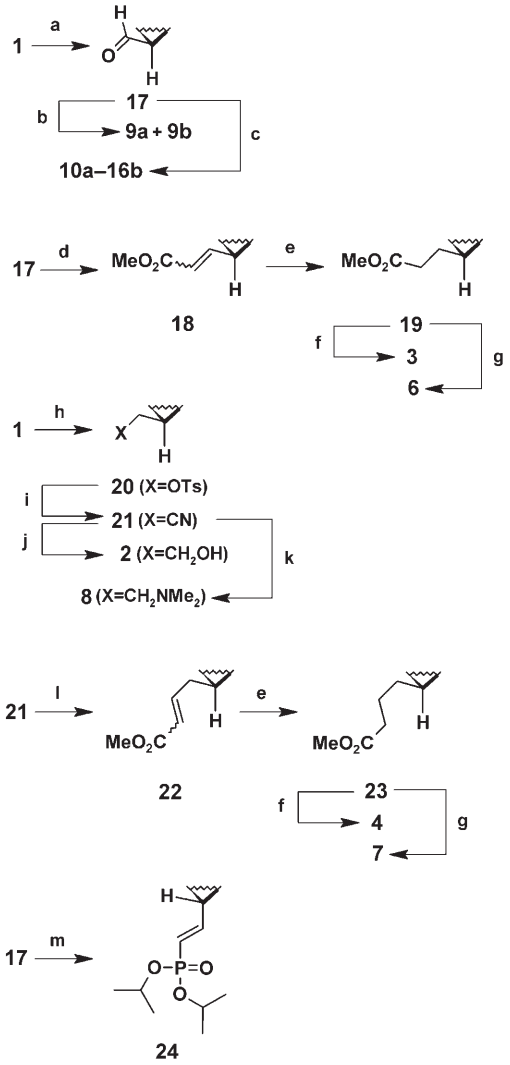

Scheme 1. Reagents and conditions: a) IBX, DMSO, RT, 4 h, quantitative; b) $BrCH_2CO_2Et$, Mn, Cp_2TiCl_2, THF, 0 °C→RT, 19 h, 99% (crude product); c) RMgX, Et_2O or THF, 0 °C→RT, 0.5–2.5 h, 67–96%; d) $Ph_3P{=}CHCO_2Me$, CH_2Cl_2, reflux, 83% e) H_2, Pd/C, EtOH, overnight, 96–98%; f) $LiAlH_4$, THF, 0 °C→RT, 1 h, 84–94%; g) NaOH, THF/water, 60 °C, overnight, 90–91%; h) TsCl, Et_3N, DMAP, CH_2Cl_2, 0 °C→RT, 18 h, 91%; i) NaCN, NaI, DMSO, 90 °C, 21 h, 64%; j) DIBALH, CH_2Cl_2, 0 °C, 1 h, then $NaBH_4$, MeOH, 0 °C, 1 h, 83% (2 steps); k) DIBALH, CH_2Cl_2, 0 °C, 2 h, then $[IrCl(cod)]_2$, Me_2NH, Et_3SiH, 1,4-dioxane, 85 °C, overnight, 61% (1 step); l) DIBALH, CH_2Cl_2, 0 °C, then $Ph_3P{=}CHCO_2Me$, CH_2Cl_2, reflux, 7 h, 79%; m) $(iPr_2O_3P)_2CH_2$, NaH, THF, 0 °C→RT, overnight, 82%. DIBALH = diisobutylaluminum hydride, DMAP = 4-dimethylaminopyridine.

agent (RMgX). If the Grignard reagent was used at <5 equivalents, pronounced reduction of the aldehyde **17** occurred, and longifolol (**1**) was obtained in yields up to 70%. In contrast, if compound **17** was slowly added to a solution containing 5 equivalents RMgX, the side reaction was suppressed, and the desired secondary alcohols were obtained in moderate to excellent yield. The steric demand of the alkyl substituent had a significant influence on the yields of the epimeric secondary alcohols. The product ratio of the phenyl-substituted derivatives **16a** and **16b** was 9:1, whereas that of **12a** and **12b** was 2.7:1. The formation of the *tert*-butyl-substituted derivative **15a** in particular was highly favored over its epimer **15b** because **15a** was obtained in significantly higher yield (81%) than **15b** (4.1%). All diastereomeric alcohols were readily separated by flash chromatography, and the faster-eluting epimer was obtained in higher yields in each case (the faster-eluting diastereomers are denoted by **a**; Figure 1). Notably, the epimers of the **a** series were always favored over the formation of the corresponding stereoisomers of the **b** series.

The homologous carboxylic acids **6** and **7** as well as the primary alcohols **3** and **4** were synthesized from the corresponding aldehydes in three steps: 1) Wittig reaction, 2) Pd/C-catalyzed hydrogenation, and 3) ester hydrolysis to the acids **6** and **7** or reduction with $LiAlH_4$ to the alcohols **3** and **4**. The *E*/*Z* ratio after Wittig reaction for the α,β-unsaturated ester **18** was 5:1, and that for **22** was 11:1. The tertiary amine **8** was prepared by reductive alkylation using triethylsilane as the reducing agent in the presence of an iridium catalyst.[18] The use of sodium cyanoborohydride or sodium triacetoxyborohydride as reducing agents did not furnish the expected amine. Instead, the corresponding alcohol **2** was isolated as the only product. The syntheses of further homologous primary, secondary, and tertiary amines failed as a result of the instability of the respective aldehydes, even though numerous protocols under various reaction conditions were tested. The attempt to obtain phosphonic acid derivatives from longifolylaldehyde (**17**) that could serve as mimics of carboxylic acids failed due to quantitative epimerization at C8.[19] Thus, the epimerized α,β-unsaturated diisopropyl phosphonate **24** was the only product obtained.

Stereochemistry

The absolute configuration at C1′ in the secondary alcohols **12b** and **14b** was assigned by X-ray crystallography (Figure 2). By conducting 1D and 2D NMR experiments—^1H NMR, ^{13}C NMR, gNOESY, gHMBC, gCOSY, and gHSQC—it became evident that the absolute configuration at C1′ could be determined by ^1H–^{13}C gHSQC and ^1H–^1H NOE correlations. In this respect, it should be mentioned that the corresponding NOE correlations were often difficult to assign due to signal overlap, and therefore gHSQC analysis was found to be superior be-

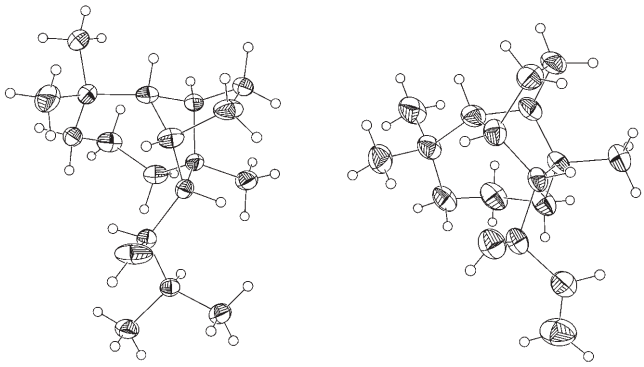

Figure 2. ORTEP plot (50% probability level) of the molecular structures of **12b** (right) and **14b** (left).

cause all the signals were resolved (detailed data and sample spectra are given in the Supporting Information).

The absolute configuration at C1′ was assigned by comparing the proton chemical shifts (^{1}H NMR δ) of the *endo*-positioned H atom in position 6, designated *endo*-C6*H*, and that of the H atom at the bridgehead in position 9, C9*H*, of one secondary alcohol to those of its respective epimer (Figure 3). NMR

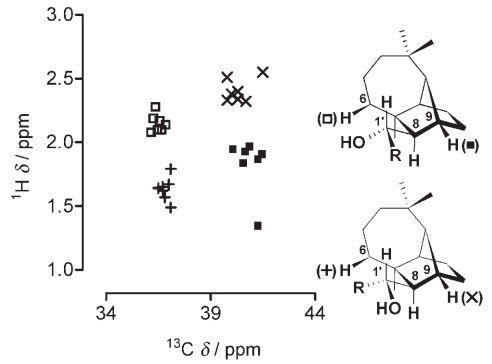

Figure 3. ^{1}H–^{13}C gHSQC correlation analysis. The ^{1}H NMR δ values (ordinate) and the ^{13}C NMR δ values (abscissa) for C6H (+, □) and C9H (×, ■) are shown. The differences in the ^{1}H NMR δ values enabled the determination of the absolute configuration, which is in agreement with X-ray crystallographic data and NOE correlations (see Supporting Information). The data for the epimers **15a** and **15b** are not displayed. Detailed gHSQC data along with sample spectra are given in the Supporting Information.

analysis showed that when the hydroxy group was oriented toward C9*H*, its ^{1}H NMR δ value was 2.32–2.55 ppm, whereas the δ value for *endo*-C6*H* was 1.49–1.79 ppm. In contrast, when the hydroxy group was in proximity with *endo*-C6*H*, its ^{1}H NMR δ value was 2.07–2.27 ppm, whereas that for C9*H* was 1.34–1.96 ppm (Figure 3 and Supporting Information). These differences were due to the close proximity of the hydroxy group and the substituent R to either C9*H* or *endo*-C6*H* (~2.50 Å in the crystal structures), resulting in different chemical environments and distinct proton chemical shift values. The carbon atoms C9 and C6 were readily identified because the ^{13}C NMR δ values were not significantly influenced by the spatial arrangement of the substituents. The arrangement of C8*H* to C1′*H* was antiperiplanar in the epimeric alcohols (dihedral angle $\phi \sim 171^\circ$) as can be observed from the crystal structures, and consistently, the coupling constants determined from ^{1}H NMR and gHSQC experiments were >10 Hz (Supporting Information).

However, the *tert*-butyl-substituted alcohol **15a** displayed a significantly smaller $^3J_{HH}$ value of 3.5 Hz for C1′*H* and C8*H*. This small $^3J_{HH}$ indicated a significant deviation from the antiperiplanar orientation and stemmed presumably from an anticlinal arrangement of C8*H* to C1′*H* ($\phi \sim 120^\circ$). In contrast, its epimer **15b** displayed a $^3J_{HH}$ value of 11.0 Hz, indicating that the antiperiplanar orientation was retained in this compound. The absolute configuration at C1′ and the spatial arrangement of the substituents are proposed as displayed in Figure 4 based on 1D and 2D NMR analysis (Supporting Information).

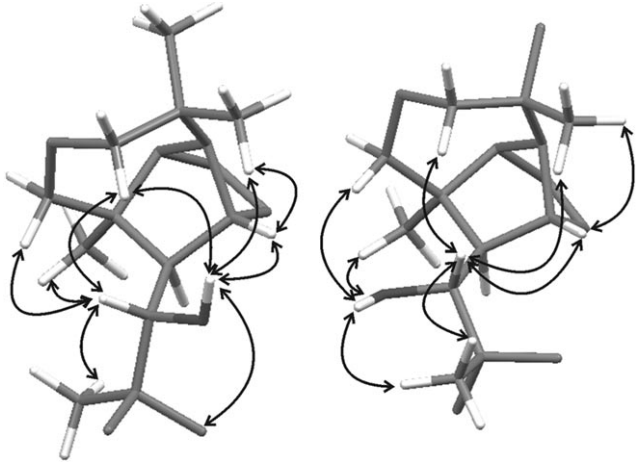

Figure 4. Proposed configuration at C1′ for **15a** (left) and its epimer **15b** (right) based on 1D and 2D NMR analysis. NOE correlations for C1′O*H*, C1′*H*, and C9*H* are displayed. The small $^3J_{HH}$ value of 3.5 Hz indicated an anticlinal arrangement of C1′*H* to C8*H* for **15a** due to the steric demand exerted by its bulky *tert*-butyl substituent. However, the antiperiplanar orientation is presumably retained in its stereoisomer **15b** ($^3J_{HH} = 11.0$ Hz).

The steric hindrance exerted by the tricyclic hydrocarbon framework results in highly impaired rotation along the C1′–C8 σ bond. Hence, the spatial orientation of the hydroxy group and the substituent R at C1′ is rather well defined. This conformational restriction might be partly responsible for the great differences in the measured ^{1}H NMR δ values that allowed the assignment of the absolute configuration at C1′. It is also noteworthy that the epimer in which the hydroxy group was pointing toward *endo*-C6*H* possessed a higher R_f value than its corresponding stereoisomer and eluted from the chromatography column first. In the case of the *tert*-butyl-substituted derivatives **15a** and **15b**, however, compound **15b**, in which the OH group is pointing toward *endo*-C6*H*, had a smaller R_f value than **15a** and eluted from the column later.

Inhibitory activity

The decrease in the rate of the UGT2B7-catalyzed estriol glucuronidation (% inhibition) in the presence of each longifolol derivative was measured. The IC_{50} value was calculated from this data and was applied to estimate the affinity for each terpenoid derivative toward the enzyme (Tables 1 and 2). Estriol was chosen as the reference substrate because this steroid displayed simple Michaelis–Menten kinetics without substrate inhibition, and the enzyme assays displayed good reproducibility. Furthermore, estriol β-D-glucuronide was conveniently detected by fluorescence spectroscopy. The % inhibition exerted by the substrate longifolol (**1**) was applied as a reference to indicate high affinity. The competitive inhibition constant (K_{ic}) of longifolol was previously determined by our research group to be 23 nM.[13]

Table 1 presents the results of the screening assays for the homochiral derivatives shown in Figure 1. The IC_{50}^{calc} values ranged between 100 nM and 13 μM, and some general trends were observed. The introduction of hydrophilic and potentially

Table 1. Inhibition levels exerted by the homochiral derivatives.

Compd	Inhibition [%][a]				IC_{50}^{calc} [μM][b]
	100 μM	10 μM	1.0 μM	0.1 μM	
primary alcohols					
1	100	100	85	51*	0.1
2	100	96	81*	27*	0.3
3	97	97	56*	11	0.8
4	100	88	46*	10	1
carboxylic acids					
5	98	93	69*	19*	0.4
6	100	92	48*	8	1
7	87	43*	10	0	13
tertiary amine					
8	95	77*	24*	5	3

[a] The % inhibition was measured at a constant estriol concentration of 25 μM. The inhibitor concentrations are indicated. [b] $IC_{50}^{calc} = [(100/\%\,\text{inhibition}) - 1] \times [\text{inhibitor}]$; IC_{50}^{calc} determined from the value(s) marked by an asterisk.[26] The IC_{50} value of longifolol was previously determined (74 nM).[13]

Table 2. Inhibition levels exerted by the epimeric derivatives.

Compd	Inhibition [%][a]				IC_{50}^{calc} [μM][b]
	100 μM	10 μM	1.0 μM	0.1 μM	
9a	100	91	70*	14*	0.5
9b	98	94	68*	16*	0.5
10a	98	99	87	47*	0.1
10b	100	98	92	63*	0.06
11a	98	98	95	57*	0.08
11b	99	99	98	76*	0.03
12a	97	99	95	59*	0.07
12b	100	100	99	83*	0.02
13a	100	97	95	72*	0.04
13b	100	96	98	84*	0.02
14a	100	98	98	73*	0.04
14b	100	98	97	91*	0.01
15a	96	81*	26*	0	3
15b	98	92	63*	16*	0.6
16a	100	97	95	56*	0.08
16b	100	100	98	96*	0.004

[a] The % inhibition was measured at a constant estriol concentration of 25 μM. The inhibitor concentrations are indicated. [b] $IC_{50}^{calc} = [(100/\%\,\text{inhibition}) - 1] \times [\text{inhibitor}]$; IC_{50}^{calc} determined from the value(s) marked by an asterisk.[26] The IC_{50} value of longifolol was previously determined (74 nM).[13]

charged substituents such as carboxy and amino groups resulted in lower affinities toward UGT2B7. Hence, these groups presumably did not exhibit significant attractive interactions toward the binding site of UGT2B7 to promote affinity. The carboxylic acid **7** displayed the highest IC_{50}^{calc} value (13 μM), which is 13-fold higher than that of its alcohol derivative **4**. Moreover, the elongation of the side chain in both alcohol and acid derivatives resulted in lower affinities toward UGT2B7. This stemmed presumably from the higher flexibility of the longer side chain leading to an increased entropy cost during the formation of the enzyme–inhibitor complex. Hence, the alcohol **4** and the carboxylic acid **7** displayed the highest IC_{50}^{calc} values within the set of homologous alcohols and carboxylic acids, respectively. The substrate longifolol (**1**) was the best inhibitor within the set of monofunctional derivatives. Therefore, it was assumed that the OH group at C1′ promoted affinity toward the enzyme.

To clarify whether or not the OH group at C1′ is crucial for high affinity, various compounds were synthesized in which this nucleophilic group was retained (Figure 2). For this study, only lipophilic substituents were attached to the side chain of longifolol owing to the observed low affinities, which resulted from the introduction of hydrophilic substituents (Table 1). The introduction of a second substituent to the diastereotopic C1′ in longifolol (**1**) resulted in two stereoisomers, which were related as epimers (Figure 2). The results of the screening assays showed that lipophilic substituents increased the affinity toward UGT2B7 because most of the compounds displayed IC_{50}^{calc} values $\leq$100 nM (Table 2). Only the β-hydroxy esters (**9a**, **9b**) and the *tert*-butyl-substituted secondary alcohols (**15a**, **15b**) exerted lower affinity than the reference compound longifolol (**1**) within this set of epimers. The lower affinity exerted by the derivatives **9a** and **9b** stemmed presumably from the higher hydrophilicity of the polar ester group in comparison with the highly lipophilic alkyl substituents. The significantly lower affinity exerted by the derivatives **15a** and **15b** that possess the bulky *tert*-butyl group was remarkable because the isopropyl- (**14a**, **14b**) and phenyl-substituted epimers (**16a**, **16b**) displayed significantly lower IC_{50}^{calc} values. Clearly, the sterically demanding *tert*-butyl group induced repulsive interactions toward the binding site of UGT2B7 that were not encountered during the formation of the enzyme complex with the derivatives bearing isopropyl and phenyl groups.

Most of the epimers of each compound displayed highly similar IC_{50}^{calc} values, indicating that the spatial orientation of the OH group and thus the configuration at C1′ had no significant influence on the affinity toward UGT2B7. This finding was consistent with our previously published results that the spatial arrangement of the OH group has no effect on the formation of the protein–ligand complex.[7] However, the epimeric secondary alcohols **16a** and **16b** displayed significantly different affinities because the IC_{50}^{calc} value of **16b** was 20-fold higher than that of **16a**. This might result from specific attractive lipophilic interactions between the phenyl group toward the binding site of UGT2B7. Therefore, we concluded that the spatial arrangement of the phenyl group had a significant effect on the inhibition level, indicating a spatially defined interaction between the inhibitor and the binding site of the enzyme. In this respect, the phenyl-substituted derivative **16b** was the best inhibitor ($IC_{50}^{calc} = 4$ nM) and was therefore chosen for further studies.

The apparent high affinity of compound **16b** toward the binding site of UGT2B7 was confirmed by measuring its IC_{50} value under the same conditions of the screening assay. The IC_{50} of the phenyl-substituted derivative **16b** was 6.3 nM (standard deviation (SD) = 0.47, $n = 15$; $CI_{95\%} = 5.3$–7.3), which was in good agreement with the IC_{50}^{calc} value (4 nM). Therefore, compound **16b** was a potent inhibitor of the UGT2B7-catalyzed estriol glucuronidation. Due to its high affinity, the rever-

sibility of inhibition was measured to determine whether or not the compound was a tight-binding, slowly reversible inhibitor. The reversibility of inhibition was assessed according to standard procedures by measuring the recovery of enzymatic activity after a rapid and large dilution (Supporting Information). The secondary alcohol **16b** displayed the expected behavior of a rapidly reversible inhibitor, and standard assays using initial rate measurements could be used for further kinetic studies.

The mode of inhibition—either competitive, uncompetitive, noncompetitive, or mixed-type—was determined by measuring the effects of the [S]/K_M ratio of estriol on the apparent IC_{50} values of the terpenoid alcohol **16b**. The % inhibition exerted by the competitive inhibitor longifolol (**1**) was employed as control. As can be observed from Figure 5, the compound displayed competitive, active-site-directed inhibition because the corresponding IC_{50} values increased linearly with increasing concentration of the reference substrate estriol.

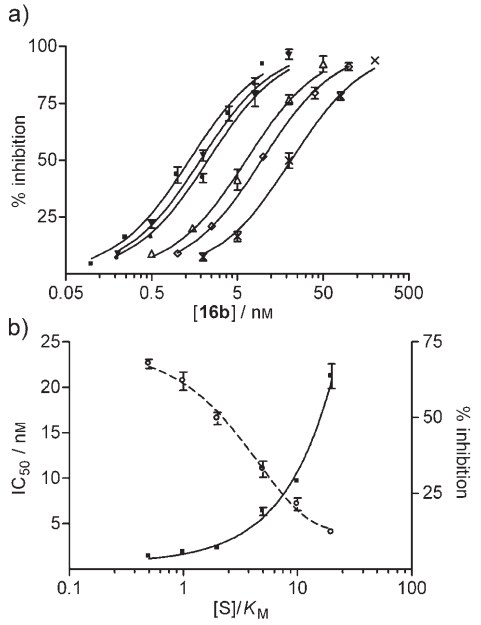

Figure 5. Effect of the [S]/K_M ratio of estriol on the IC_{50} value of **16b** to determine the mode of inhibition. Panel a) shows the data of each IC_{50} determination. Panel b) displays the IC_{50} values of **16b** as a function of the [S]/K_M ratio of the reference substrate estriol ($r^2 = 0.993$, left ordinate, solid line, ■). The dashed line displays the results of the control assays using the competitive inhibitor longifolol (**1**) at a fixed concentration of 0.10 μM at each [S]/K_M ratio (right ordinate, ○). The mean and SD values are displayed: a) $n = 3$, b) $n = 15$ for IC_{50} values; $n = 3$ for control assays. The [S]/K_M ratios are plotted on a logarithmic scale for clarity. Compound **16b** displayed the expected behavior for a competitive inhibitor.

The competitive inhibition constant was measured to confirm the high affinity and the mechanism of inhibition exerted by the inhibitor as indicated by the studies described above. Furthermore, the K_{ic} value of the secondary alcohol **16b** was determined to derive a kinetic parameter that is independent of substrate concentration. The data were fitted by simultaneous nonlinear regression to the competitive, noncompetitive, mixed-type, and uncompetitive inhibition models, which were ranked according to the corrected Akaike's information criterion (results not shown).[20] Based on this analysis, the active-site-directed, competitive inhibition model was chosen, and the resulting K_{ic} was consistent with the expected value, which was calculated from its IC_{50} (Cheng–Prusoff equation). The very low K_{ic} value of 0.91 nM confirmed the high affinity of compound **16b** toward UGT2B7 (Figure 6).

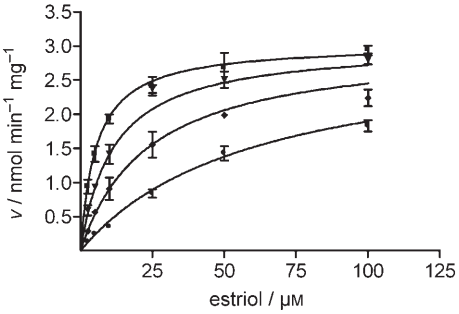

Figure 6. Determination of the K_{ic} value of inhibitor **16b** assayed with UGT2B7. The mean and SD values are shown ($n = 3$). The K_{ic} value for the UGT2B7-catalyzed estriol glucuronidation was 0.91 nM (SD = 0.071, $n = 72$; $CI_{95\%} = 0.76$ to 1.0).

The inhibitor **16b** was employed to assess its inhibitory activity toward the glucuronidation of structurally different substrates of UGT2B7. Its substrate-independent inhibition was assessed by measuring the IC_{50} value of the secondary alcohol **16b** towards five different substrates of UGT2B7, namely 1-naphthol, 4-nitrophenol, scopoletin, epitestosterone, and 4-methylumbelliferone. The measured IC_{50} values ranged from 3.4 to 6.3 nM (SD < 11.3 %, $n = 15$) and confirmed that the high inhibition exerted by **16b** was independent of the substrate employed.

It was determined that compound **16b** was not conjugated by UGT2B7 by conducting assays with [^{14}C]UDPGlcA. The glucuronidation assays were carried out by using the enzyme at high concentration (2.0 mg mL^{-1}) and an incubation time of 14 h in order to identify even small amounts of [^{14}C]β-D-glucuronide. The use of radiolabeled co-substrate was necessary due to the low UV absorption of compound **16b**. The results suggested that the steric hindrance in the vicinity of the OH group exerted by the bulky phenyl group prevented the enzyme-catalyzed conjugation of the nucleophilic group. Other hepatic UGT enzymes also did not conjugate the inhibitor because assays with human liver microsomes did not afford the corresponding [^{14}C]β-D-glucuronide. These findings indicated that **16b** was a true inhibitor of the enzyme. Interestingly, molecular modeling suggested that the phenyl-substituted derivative **16b** was unable to accommodate the GlcA moiety at its hydroxy group due to the steric hindrance exerted by the phenyl group in proximity to the bulky tricyclic scaffold (results not shown).

The isoform selectivity was assessed by measuring the % inhibition exerted by compound **16b** towards the glucuronidation reaction catalyzed by 14 different UGT isoforms of subfam-

ily 1A and 2B. Umbelliferone and 1-hydroxypyrene were chosen as reference substrates because these compounds are glucuronidated by many different UGT enzymes and can be conveniently analyzed by fluorescence spectroscopy. The inhibitor **16b** was employed at concentrations of 10, 25, and 50 μM, which are significantly (>1000-fold) higher than its K_{ic} toward UGT2B7. As can be observed from Figure 7, The phenyl group

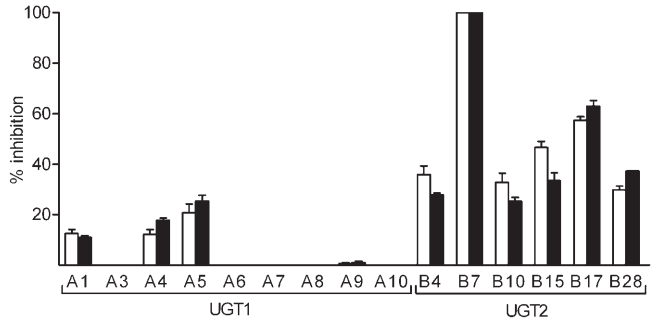

Figure 7. Inhibition of the UGT-catalyzed glucuronidation of umbelliferone and 1-hydroxypyrene by compound **1** (white bars) and inhibitor **16b** (black bars). The results for an inhibitor concentration of 25 μM are displayed. The mean and SD values are shown ($n=4$).

presumably had no effect on the isoform selectivity because the % inhibition exerted by **16b** was similar to that exerted by longifolol (**1**). Furthermore, the results indicated that the inhibitor **16b** was highly isoform selective for UGT2B7. Most of the UGT1A isoforms did not display any significant response to the inhibitor. In contrast, the activity of the UGT2B isoforms was decreased by approximately 30–70% by this high concentration of **16b**. In addition to UGT2B7, which was completely inhibited, the UGT2B17-catalyzed glucuronidation reaction displayed the highest response to the inhibitors (~70% inhibition). The isoform 2B17 was therefore chosen to assess the true selectivity of inhibitor **16b**. The K_{ic} value of **16b** for UGT2B17 was 27.6 μM (SD=2.91, $n=54$, $CI_{95\%}=23.1–32.0$), and the true selectivity ($K_{ic}^{2B17}/K_{ic}^{2B7}$) of this inhibitor for UGT2B7 was therefore >20000. The large difference in the K_{ic} values was confirmed by measuring the inhibitory activity of **16b** toward the UGT2B7- and UGT2B17-catalyzed glucuronidation of their common substrates 1-naphthol and 4-methylumbelliferone (results not shown).

Conclusions

The presented results indicate that the phenyl-substituted longifolol derivative **16b** (β-phenyllongifolol) is a highly selective inhibitor of the UGT2B7-catalyzed glucuronidation reaction.[21] The apparent preferential inhibition of UGT2B7 is remarkable considering the promiscuous character of metabolic enzymes. The tricyclo[5.4.0.0^{2,9}]undecane framework is presumably responsible for the isoform selectivity. The tricyclic hydrocarbon scaffold together with the phenyl group promote affinity toward UGT2B7. Furthermore, the phenyl group increases the steric hindrance in proximity of the hydroxy group to decrease the accessibility to this nucleophilic functionality to prohibit enzymatic glucuronidation. The hydroxy group presumably has no significant effect on the formation of the enzyme–inhibitor complex, indicating that there is no significant attractive interaction to the binding site of UGT2B7. The OH group merely promotes water solubility. Furthermore, the very low K_{ic} value of 0.91 nM is remarkable because UGTs are commonly described as flexible enzymes that generally do not display low dissociation constants. This low inhibitory dissociation constant indicates specific attractive interactions toward the binding site of UGT2B7. Therefore, the formation of the encounter complex seems to be controlled by mere hydrophobic interactions.

Experimental Section

Materials. UDPGlcA (trisodium salt, CAS 63700-19-6), saccharic acid-1,4-lactone (CAS 61278-30-6), estriol (CAS 50-27-1), scopoletin (CAS 92-61-5), 4-methylumbelliferone (CAS 90-33-5), and epitestosterone (CAS 481-30-1) were obtained from Sigma (St. Louis, MO, USA). 4-Nitrophenol (CAS 100-02-7), 1-naphthol (CAS 90-15-3), and umbelliferone (CAS 93-35-6) were from Aldrich (Schnelldorf, Germany). Radiolabeled [^{14}C]UDPGlcA was acquired from PerkinElmer Life and Analytical Sciences (Boston, MA, USA). HPLC-grade solvents were used throughout the study. The recombinant human UGTs were expressed as His-tagged proteins in baculovirus-infected insect cells as previously described.[22] The cDNA for the human UGT2B17 was a generous gift from Professor Peter Mackenzie (Flinders University, Flinders Medical Centre, Bedford Park, South Australia, Australia).

Syntheses. The procedures for the syntheses and the characterization of the compounds are given in the Supporting Information.

X-ray crystal structures. Crystallographic data for the X-ray measurements of **12b** and **14b** are given in the Supporting Information. Data were collected on a Oxford Gemini S diffractometer ($Cu_{K\alpha}$ radiation, $\lambda=1.54248$ Å) at 100 K. All structures were solved by direct methods (SHELXS-97)[23] and refined by full-matrix least-squares methods against F^2 (SHELXL-97).[24] All non-hydrogen atoms were refined anisotropically. All hydrogen atom positions, except O-bonded hydrogen atoms in the case of **12b**, were refined using a riding model. The positions of O-bonded hydrogen atoms of **12b** were taken from the difference Fourier map and refined isotropically. The absolute structures were determined with respect to the Flack parameter.[25]

Inhibitor screening. The % inhibition was measured at four inhibitor concentrations (0.10, 1.0, 10, and 100 μM) using estriol as the reference substrate (25 μM). The reaction mixture consisted of phosphate buffer (50 mM, pH 7.4), $MgCl_2$ (10 mM), and saccharic acid-1,4-lactone (5.0 mM). The concentration of UGT2B7 was 0.10 mg mL^{-1}. Assays in the absence of inhibitor, blank runs in the absence of co-substrate, and control assays employing longifolol (**1**) were included in each assay. The enzyme reaction was initiated by the addition of a solution of UDPGlcA to a final concentration of 5.0 mM. The enzyme reactions were terminated after an incubation time of 15 min at 37 °C by the addition of ice-cold perchloric acid (4.0 M) and transfer to ice. The mixtures were centrifuged (16000 *g*, 10 min) and aliquots of the supernatants were subjected to HPLC analysis. The results reflect a minimum of three replicate determinations.

IC_{50} values. The IC_{50} values of compound **16b** were determined at five concentrations bracketing its apparent IC_{50} value (0.10, 0.25, 1.0, 4.0, and $10\times IC_{50}$). Estriol was employed at six $[S]/K_M$ ratios (0.5, 1.0, 2.0, 5.0, 10, and 20). The reaction mixture consisted of phosphate buffer (50 mM, pH 7.4), $MgCl_2$ (10 mM), and saccharic acid-1,4-lactone (5.0 mM). The enzyme UGT2B7 was used at 0.10 mg mL^{-1}. Assays in the absence of inhibitor, blank runs in the absence of co-substrate, and control assays using longifolol (**1**) at a fixed concentration of 0.10 μM were included at each $[S]/K_M$ ratio. The enzyme reaction was initiated after a pre-incubation time of 5 min at 37 °C by the addition of a solution of UDPGlcA to a final concentration of 5.0 mM. The enzyme reactions were terminated after an incubation time of 15 min at 37 °C by the addition of ice-cold perchloric acid (4.0 M) and transfer to ice. The mixtures were centrifuged (16000 *g*, 10 min), and aliquots of the supernatants were subjected to HPLC analysis. The data were analyzed by nonlinear regression applying the two-parameter Hill equation. The results reflect a minimum of three replicate determinations.

Testing for reversibility. UGT2B7 at a concentration of 5.0 mg mL^{-1} was pre-incubated in buffered solution (phosphate buffer, 50 mM, pH 7.4) at 37 °C with a concentration of **16b** equivalent to 10-fold its IC_{50}. After an equilibration time of 45 min, this mixture was diluted 100-fold into reaction buffer (37 °C) containing the reference substrate estriol (25 μM), phosphate buffer (50 mM, pH 7.4), UDPGlcA (5.0 mM), $MgCl_2$ (10 mM), and saccharic acid-1,4-lactone (5.0 mM) to initiate reaction. The formation of glucuronide was monitored every 2.5 min over 60 min by pipetting 100 μL of the reaction buffer to a vial containing 10 μL perchloric acid (4.0 M). The acidified mixtures were transferred to ice, centrifuged (16000 *g*, 10 min), and aliquots of the supernatants were subjected to HPLC analysis. Control assays in the absence of terpenoid alcohol were included. The results reflect a minimum of two replicate determinations (Supporting Information).

Inhibitory dissociation constants. The K_{ic} value for UGT2B7 (0.10 mg mL^{-1}) was determined at six estriol concentrations (2.5, 5.0, 10, 25, 50, and 100 μM), and the inhibitor **16b** was employed at three concentrations (1.0, 3.0, and 9.0 nM). The K_{ic} value for UGT2B17 (0.15 mg mL^{-1}) was measured at six scopoletin concentrations (25, 50, 100, 250, 500, and 1000 μM), and compound **16b** was used at concentrations of 10 and 25 μM. Estriol assay: The enzyme reactions were initiated after a pre-incubation time of 5 min at 37 °C by the addition of a solution of UDPGlcA to a final concentration of 5.0 mM. The enzyme reactions were terminated after an incubation time of 15 min at 37 °C by the addition of ice-cold perchloric acid (4.0 M) and transfer to ice. The mixtures were centrifuged (16000 *g*, 10 min), and aliquots of the supernatants were subjected to HPLC analysis. The results reflect a minimum of three replicate determinations. Scopoletin assay: The enzyme reactions were initiated after a pre-incubation time of 5 min at 37 °C by the addition of a solution of UDPGlcA to a final concentration of 5.0 mM. The enzyme reactions were terminated after an incubation time of 10 min at 37 °C by the addition of ice-cold perchloric acid (4.0 M) and transfer to ice. The mixtures were centrifuged (16000 *g*, 10 min), and aliquots of the supernatants were subjected to HPLC analysis. The results reflect a minimum of three replicate determinations.

Testing for substrate-independent inhibition. The IC_{50} values of inhibitor **16b** were determined by the use of five different reference substrates. The assay conditions were balanced using the substrates at concentrations that resembled their K_M values for UGT2B7: 1-naphthol (300 μM, 0.20 mg protein mL^{-1}, incubation time 20 min), 4-nitrophenol (500 μM, 0.10 mg protein mL^{-1}, incubation time 10 min), scopoletin (320 μM, 0.10 mg protein mL^{-1}, incubation time 10 min), epitestosterone (15 μM, 0.25 mg protein mL^{-1}, incubation time 20 min), and 4-methylumbelliferone (600 μM, 0.20 mg protein mL^{-1}, incubation time 20 min). Compound **16b** was employed at five concentrations bracketing its IC_{50} value (0.10, 0.25, 1.0, 4.0, and $10\times IC_{50}$). The assays were carried out as described above. The results reflect a minimum of two replicate determinations.

Isoform selectivity. Umbelliferone (100 μM) was used as the substrate for the UGT isoforms 1A1 (0.15 mg mL^{-1}), 1A7 (0.15 mg mL^{-1}), 1A8 (0.11 mg mL^{-1}), 1A9 (0.15 mg mL^{-1}), 1A10 (0.12 mg mL^{-1}), and 2B7 (0.10 mg mL^{-1}). The UGTs 1A3 (0.40 mg mL^{-1}), 1A4 (0.50 mg mL^{-1}), 1A5 (0.11 mg mL^{-1}), 1A6 (0.10 mg mL^{-1}), 2B4 (0.50 mg mL^{-1}), 2B10 (0.26 mg mL^{-1}), 2B15 (0.50 mg mL^{-1}), 2B17 (0.20 mg mL^{-1}), and 2B28 (0.25 mg mL^{-1}) were assayed using 1-hydroxypyrene (50 μM). Longifolol (**1**) and the inhibitor **16b** were employed at concentrations of 10, 25, and 50 μM. The enzyme reactions were initiated after a pre-incubation time of 5 min at 37 °C by the addition of a solution of UDPGlcA to a final concentration of 5.0 mM. Umbelliferone assays: The enzyme reactions were terminated after an incubation time of 25 min at 37 °C by the addition of ice-cold perchloric acid (4.0 M) and transfer to ice. The mixtures were centrifuged (16000 *g*, 10 min), and aliquots of the supernatants were subjected to HPLC analysis. 1-Hydroxypyrene assays: The enzyme reactions were terminated after an incubation time of 20 min at 37 °C by the addition of ice-cold aqueous $ZnSO_4$ (15% by weight), followed by acetonitrile, and transfer to ice. The mixtures were centrifuged (16000 *g*, 10 min), and aliquots of the supernatants were subjected to HPLC analysis. The results reflect a minimum of four replicate determinations.

Glucuronidation assays. The formation of glucuronide was assayed by the use of radiolabeled [^{14}C]UDPGlcA. A solution of [^{14}C]UDPGlcA (400 μL, 196 mCi mmol^{-1}, 0.02 mCi mL^{-1} in EtOH/water 7:1 *v/v*) was transferred to 2-mL vials, and the solvent was evaporated in vacuo at room temperature. The residue was dissolved in reaction buffer (90 μL), which consisted of either UGT2B7 (2.0 mg mL^{-1}) or human liver microsomes (100 μg), $MgCl_2$ (10 mM), phosphate buffer (50 mM, pH 7.4), and saccharic acid-1,4-lactone (5.0 mM). A solution of inhibitor **16b** (1.0 mM in 50-vol% DMSO/water) was added to the reaction buffer to a final saturating concentration of 100 μM ($\sim 5500\times K_{ic}^{2B7}$). After incubating for 14 h at 37 °C, the reaction mixture was centrifuged (16000 *g*, 10 min), and aliquots of the supernatants were subjected to HPLC analysis. Control assays in the presence of the substrate longifolol (100 μM) and blank runs were included. The detection limit (30 pmol, signal-to-noise ratio = 10:1) was determined by subjecting dilutions of reaction buffer containing longifolol [^{14}C]β-D-glucuronide to HPLC analysis. The results reflect a minimum of two replicate determinations.

HPLC methods. The HPLC system consisted of the Agilent 1100 series degasser, binary pump, autosampler, thermostat-controlled column compartment, multiple-wavelength detector, and fluorescence detector (Agilent Technologies, Palo Alto, CA, USA). The resulting spectra were analyzed with Agilent ChemStation software (Rev B.01.01). Glucuronidation reaction products were separated and detected as follows. Estriol β-D-glucuronide: Hypersil BDS-C18 (150×4.6 mm, Agilent Technologies, Palo Alto, CA, USA); 35% MeOH in phosphate buffer (50 mM, pH 3.0); flow rate 1.0 mL min^{-1}; detection by fluorescence spectroscopy (λ_{ex} = 335 nm, λ_{em} = 455 nm); t_R = 4.2 min. 4-Nitrophenol β-D-glucuronide: Chromolith SpeedROD (50×4.6 mm, Merck, Darmstadt, Germany); 15% acetonitrile in phosphate buffer (50 mM, pH 3.0); flow rate 1.0 mL min^{-1}; detection by UV spectroscopy (λ = 300 nm); t_R = 1.3 min. Scopoletin

β-D-glucuronide: Chromolith SpeedROD (50×4.6 mm); 10% MeOH in phosphate buffer (50 mM, pH 3.0); flow rate (gradient run) 0.8 mL min^{-1} (0.0 to 4.5 min), 0.8 mL→2.5 mL min^{-1} (4.5 to 5.0 min), 2.5 mL min^{-1} (5.0 to 11.0 min), 2.5→0.8 mL min^{-1} (11.0 to 12 min); detection by fluorescence spectroscopy (λ_{ex}=335 nm, λ_{em}=455 nm); t_R=4.2 min. Epitestosterone β-D-glucuronide: Chromolith SpeedROD (50×4.6 mm); 43% MeOH in phosphate buffer (50 mM, pH 3.0); flow rate 2.0 mL min^{-1}; detection by UV spectroscopy (λ=246 nm); t_R=5.9 min. 1-Naphthol β-D-glucuronide: Hypersil BDS-C18 (150×4.6 mm); 42% MeOH in phosphate buffer (50 mM, pH 3.0); flow rate 1.0 mL min^{-1}; detection by fluorescence spectroscopy (λ_{ex}=285 nm, λ_{em}=335 nm); t_R=4.9 min. Umbelliferone β-D-glucuronide: Chromolith SpeedROD (50×4.6 mm); 15% MeOH in phosphate buffer (50 mM, pH 3.0); flow rate 1.5 mL min^{-1}; detection by fluorescence spectroscopy (λ_{ex}=316 nm, λ_{em}=382 nm); t_R=1.4 min. 4-Methylumbelliferone β-D-glucuronide: Chromolith SpeedROD (50×4.6 mm); 20% MeOH in phosphate buffer (50 mM, pH 3.0); flow rate 2.0 mL min^{-1}; detection by fluorescence spectroscopy (λ_{ex}=316 nm, λ_{em}=382 nm); t_R=1.3 min. 1-Hydroxypyrene β-D-glucuronide: Hypersil BDS-C18 (150×4.6 mm); 40% acetic acid (0.5-vol%) in acetonitrile; flow rate 0.9 mL min^{-1}; detection by fluorescence spectroscopy (λ_{ex}=237 nm, λ_{em}=388 nm); t_R=2.3 min. [^{14}C]β-D-Glucuronides: Chromolith SpeedROD (50×4.6 mm); gradient run 5% MeOH in phosphate buffer (50 mM, pH 3.0; 0.0 to 3.5 min), 5%→80% MeOH (3.5 to 8.0 min), 80% MeOH (8.0 to 13 min), 80%→5% MeOH (13 to 15 min), 5% MeOH (15 to 20 min); flow rate 1.0 mL min^{-1}; retention time for longifolol [^{14}C]β-D-glucuronide 9.5 min; detection with a 9701 HPLC radioactivity monitor (Reeve Analytical, Glasgow, Scotland).

Acknowledgements

The authors thank Sirkku Jäntti for conducting the LC–MS analyses. This work was supported by a fellowship from the Finnish Cultural Foundation (I.B.), a grant from Walter och Lisi Wahls Stiftelse för Naturvetenskaplig Forskning, and the Academy of Finland (projects 207535 and 210933).

Keywords: eudismic analysis · inhibition · metabolism · UGT

[1] For reviews, see: a) A. Radominska-Pandya, M. Ouzzine, S. Fournel-Gigleux, J. Magdalou, *Methods Enzymol.* **2005**, *400*, 116–147; b) P. G. Wells, P. I. Mackenzie, J. R. Chowdhury, C. Guillemette, P. A. Gregory, Y. Ishii, A. J. Hansen, F. K. Kessler, P. M. Kim, N. R. Chowdhury, J. K. Ritter, *Drug Metab. Dispos.* **2004**, *32*, 281–290; c) M. B. Fisher, M. F. Paine, T. J. Strelevitz, S. A. Wrighton, *Drug Metab. Rev.* **2001**, *33*, 273–297; d) C. D. King, G. R. Rios, M. D. Green, T. R. Tephly, *Curr. Drug Metab.* **2000**, *1*, 143–161.

[2] I. S. Owens, N. K. Basu, R. Banerjee, *Methods Enzymol.* **2005**, *400*, 1–22.

[3] J. A. Williams, R. Hyland, B. C. Jones, D. A. Smith, S. Hurst, T. C. Goosen, V. Peterkin, J. Koup, S. E. Ball, *Drug Metab. Dispos.* **2004**, *32*, 1201–1208.

[4] M. H. Court, *Methods Enzymol.* **2005**, *400*, 104–116.

[5] S. D. Copley, *Curr. Opin. Chem. Biol.* **2003**, 7, 265–272.

[6] a) K. H. G. Verschueren, S. M. Franken, H. J. Rozeboom, K. H. Kalk, B. W. Dijkstra, *J. Mol. Biol.* **1993**, *232*, 856–872; b) F. C. Lightstone, Z. Ya-Jun, A. H. Maulitz, T. C. Bruice, *Proc. Natl. Acad. Sci. USA* **1997**, *94*, 8417–8420; c) G. D. Markham, D. W. Parkin, F. Mentch, V. L. Schramm, *J. Biol. Chem.* **1987**, *262*, 5609–5615.

[7] J. R. Halpert, F. P. Guengerich, J. R. Bend, M. A. Correia, *Toxicol. Appl. Pharmacol.* **1994**, *125*, 163–175.

[8] K. Grancharov, Z. Naydenova, S. Lozeva, E. Golovinsky, *Pharmacol. Ther.* **2001**, *89*, 171–186.

[9] a) C. M. Timmers, M. Dekker, R. C. Buijsman, G. A. van der Marel, B. Ethell, G. Anderson, B. Burchell, G. J. Mulder, J. H. van Boom, *Bioorg. Med. Chem. Lett.* **1997**, *7*, 1501–1506; b) D. Noort, E. A. Meijer, T. J. Visser, J. H. N. Meerman; G. A. van der Marel, J. H. van Boom, G. J. Mulder, *Mol. Pharmacol.* **1991**, *40*, 316–320.

[10] a) V. L. Schramm, *Curr. Opin. Struct. Biol.* **2005**, *15*, 604–613; b) V. L. Schramm, *Annu. Rev. Biochem.* **1998**, *67*, 693–720.

[11] a) M. Said, D. Noort, J. Magdalou, J. C. Ziegler, G. A. van der Marel, J. H. van Boom, G. J. Mulder, G. Siest, *Biochem. Biophys. Res. Commun.* **1992**, *187*, 140–145; b) D. Noort, M. W. Coughtrie, B. Burchell, G. A. van der Marel, J. H. van Boom, A. van der Gen, G. J. Mulder, *Eur. J. Biochem.* **1990**, *188*, 309–312; c) D. K. Alargov, R. G. Gugova, P. S. Denkova, G. Müller, E. V. Golovinsky, *Monatsh. Chem.* **1999**, *130*, 937–943; d) D. K. Alargov, Z. Naydenova, K. Grancharov, P. S. Denkova, E. V. Golovinsky, *Monatsh. Chem.* **1997**, *128*, 725–732; e) D. K. Alargov, Z. Naydenova, K. Grancharov, P. Denkova, E. Golovinsky, *Monatsh. Chem.* **1998**, *129*, 755–760.

[12] V. Uchaipichat, P. I. Mackenzie, D. J. Elliot, J. O. Miners, *Drug Metab. Dispos.* **2006**, *34*, 449–456.

[13] I. Bichlmaier, M. Kurkela, A. Siiskonen, M. Finel, J. Yli-Kauhaluoma, *Bioorg. Chem.*, submitted.

[14] a) I. Bichlmaier, A. Siiskonen, M. Finel, J. Yli-Kauhaluoma, *J. Med. Chem.* **2006**, *49*, 1818–1827; b) I. Bichlmaier, A. Siiskonen, M. Kurkela, M. Finel, J. Yli-Kauhaluoma, *Biol. Chem.* **2006**, *387*, 407–416.

[15] C. S. Sell, *A fragrant introduction to terpenoid chemistry*, The Royal Society of Chemistry, Cambridge, **2003**, pp. 203–214.

[16] a) U. Ladziata, V. V. Zhdankin, *ARKIVOC* **2006**, *ix*, 26–58; b) M. Frigerio, M. Santagostino, S. A. Sputore, *J. Org. Chem.* **1999**, *64*, 4537–4538.

[17] J. D. Parrish, D. R. Shelton, R. D. Little, *Org. Lett.* **2003**, *5*, 3615–3617.

[18] T. Mizuta, S. Sakaguchi, Y. Ishii, *J. Org. Chem.* **2005**, *70*, 2195–2199.

[19] P. Samadder, R. Bittman, H. S. Byun, G. Arthur, *J. Med. Chem.* **2004**, *47*, 2710–2713.

[20] H. Motulsky, A. Christopoulos, *Fitting models to biological data using linear and nonlinear regression. A practical guide to curve fitting*, GraphPad Software Inc., San Diego CA, **2003**, pp. 143–146.

[21] We propose the trivial names α-phenyllongifolol and β-phenyllongifolol for compound **16a** and its epimer **16b**, respectively. The Greek letters α and β denote the relative configuration at C1′. Consistently, compound **10a** is α-methyllongifolol, its epimer **10b** is β-methyllongifolol.

[22] M. Kurkela, A. Garcia-Horsman, L. Luukkanen, S. Mörsky, J. Taskinen, M. Baumann, R. Kostiainen, J. Hirvonen and M. Finel, *J. Biol. Chem.* **2003**, *278*, 3536–3544.

[23] G. M. Sheldrick, *Acta Crystallogr. Sect. A* **1990**, *46*, 467–473.

[24] G. M. Sheldrick, SHELXL-97, A program for crystal structure refinement, Göttingen, **1996**.

[25] H. D. Flack, *Acta Crystallogr. Sect. A* **1983**, *39*, 876–881.

[26] R. A. Copeland, *Evaluation of enzyme inhibitors in drug discovery*; Wiley, Hoboken, **2005**, p. 271.

Received: October 19, 2006
Revised: March 22, 2007
Published online on May 4, 2007

